Proximity Relationships between Residue 117 of Rabbit Skeletal Troponin-I and Residues in Troponin-C and Actin

Zhixing Li,* John Gergely,*†‡ and Terence Tao*§¶

*Muscle and Motility Group, Boston Biomedical Research Institute, Watertown, Massachusetts 02472, †Neurology Service, Massachusetts General Hospital, Boston, Massachusetts 02114, ‡Department of Biological Chemistry and Molecular Pharmacology and §Department of Neurology, Harvard Medical School, Boston, Massachusetts 02115, and ¶Department of Biochemistry, Tufts University School of Medicine, Boston, Massachusetts 02111 USA

ABSTRACT We used resonance energy transfer and site-directed photo-cross-linking to probe the Ca^{2+}-dependent proximity relationships between residue 117 next to the C-terminus of the inhibitory region in rabbit skeletal troponin-I (TnI) and residues in troponin-C (TnC) and in actin. A mutant TnI that contains a single cysteine at position 117 (I117) was constructed, and the distance between TnI residue 117 and TnC residue 98 was measured with the following results: for both the binary TnC-TnI complex and the ternary troponin complex, this distance was 30 and 41 Å in the presence and absence of Ca^{2+}, respectively. The distance between TnI residue 117 and Cys374 of actin was 48 and 41 Å in the presence and absence of Ca^{2+}, respectively. Six additional distances from this TnI residue to cysteines in TnC mutants were measured and used to localize this residue with respect to the crystal structure of TnC. The results show that in the presence of Ca^{2+} it is localized near the B and C helices of TnC's N-terminal domain. In the absence of Ca^{2+} this residue moves away from this location by ~8 Å. Photo-cross-linking experiments show that I117 labeled with 4-maleimidobenzophenone photo-cross-linked to TnC but not to actin in both the presence and absence of Ca^{2+}. Taken together these results provide independent experimental support for the proposal (Y. Luo, J. L. Wu, B. Li, K. Langsetmo, J. Gergely, and T. Tao, 2000, *J. Mol. Biol.* 296:899–910) that upon Ca^{2+} removal the region comprising TnI residues 114–125 triggers the movements of residues 89–113 and 130–150 toward actin, but does not itself interact with actin.

INTRODUCTION

Troponin-I (TnI) is the inhibitory subunit of the heterotrimeric Ca^{2+}-dependent regulatory protein troponin (Tn) in the thin filaments of mammalian striated (skeletal and cardiac) muscle (see reviews by Farah and Reinach, 1995; Gordon et al., 2000; Grabarek et al., 1992; Leavis and Gergely, 1984; Perry, 1998, 1999; Tobacman, 1996). The other two Tn subunits are troponin-C (TnC) the Ca^{2+} receptor, and troponin-T (TnT), which binds tropomyosin (Tm) and serves to properly anchor TnI and TnC onto the Tm·F-actin filament. In additon, TnT may play a role in regulating the Ca^{2+}-sensitivity of S1·Tn·Tm·F-actin ATPase. TnI is capable of binding to actin and inhibiting the actomyosin ATPase by itself; this binding and inhibition is reversed by TnC in the presence of Ca^{2+}. Together with Tm, Tn is thought to regulate the interaction between myosin cross-bridges and actin in a Ca^{2+}-dependent manner, thereby controlling the contraction and relaxation of striated muscles.

TnC is composed of two protease-resistant domains, each containing two metal ion-binding E-F hand motifs. The C-terminal domain (C-domain) contains the high-affinity Ca^{2+}-binding sites that bind Mg^{2+} as well. The N-terminal domain (N-domain) contains the low-affinity Ca^{2+}-specific sites that have been shown to be the physiologically relevant activation sites (see reviews cited above). The crystal structure of TnC reveals that the two domains are linked by a long central α-helix (Herzberg and James, 1985; Sundaralingam et al., 1985). Based on this structure, it was proposed that the binding of Ca^{2+} to TnC's N-domain activation sites causes a movement of the B and C helices away from the A and D helices, exposing a hydrophobic patch that can provide an additional binding site for TnI (Herzberg et al., 1986). The occurrence of this Ca^{2+}-induced conformational transition in TnC has been verified by fluorescence (Wang et al., 1992), NMR (Gagne et al., 1995; Slupsky and Sykes, 1995), and x-ray crystallographic (Houdusse et al., 1997; Soman et al., 1999; Strynadka et al., 1997) studies. Its physiological relevance has been demonstrated using a genetically engineered disulfide bond (Grabarek et al., 1990) or salt bridge (Fujimori et al., 1990).

Early studies using TnI proteolytic fragments and synthetic peptides showed that the segment known as the inhibitory region, residues 96–115 (NQKLFDLRGKFKRPPLRRVR), can mimic a majority of the functions of TnI, viz., binding to actin, inhibiting actomyosin ATPase activity, and binding to TnC (Syska et al., 1976; Talbot and Hodges, 1981). Studies using recombinant TnI fragments showed that only those fragments that contain the inhibitory region are capable of high-affinity binding to TnC (Farah et al., 1994). A variety of other studies, most of which used recombinant or synthetic fragments, demonstrated that TnI and TnC interact with each other extensively, and in an

Received for publication 5 September 2000 and in final form 9 April 2001.

Z. Li's present address: Departments of Pediatrics and Medicine, Division of Nephrology and Hypertension, University of California, San Diego, La Jolla, CA 92093.

Address reprint requests to Dr. Terence Tao, Boston Biomedical Research Institute, 64 Grove Street, Watertown, MA 02472. Tel.: 617-658-7807; Fax: 617-972-1753; E-mail: Tao@BBRI.org.

0006-3495/01/07/321/13 $2.00

anti-parallel manner (Farah et al., 1994; Grabarek et al., 1981; Jha et al., 1996; Krudy et al., 1994; Leszyk et al., 1990; Pearlstone and Smillie, 1995; Pearlstone et al., 1997; Sheng et al., 1992). More specifically, residues 1–40 have been identified as interacting with TnC's C-domain (Farah et al., 1994; Tripet et al., 1997). Recent x-ray crystallographic studies on the complex between TnC and the TnI peptide, TnI_{1-47}, reveal that the peptide is bound in TnC's C-domain hydrophobic cleft (Vassylyev et al., 1998). Our photo-cross-linking studies using intact subunits rather than fragments revealed that TnI's inhibitory region interacts with TnC's central helix in an anti-parallel manner (Kobayashi et al., 1994, 1991; Leszyk et al., 1987, 1988). Using synthetic peptides of different lengths, Tripet et al. (1997) implicated TnI residues 116–131 (MSADAMLKALLGSKHK) as a "second TnC binding" region that interacts with TnC's N-domain in a Ca^{2+}-dependent manner. NMR studies (Li et al., 1999; McKay et al., 1997, 1998, 1999) using peptides that contain this region showed it interacts with TnC's N-domain hydrophobic cleft. Tripet et al. (1997) also implicated residues 140–148 (LKQVKKEDT) as a "second actin binding" region. From low-angle x-ray and neutron diffraction studies it was deduced that the I·C binary complex (Olah et al., 1994) and the I·C·T ternary complex (Stone et al., 1998) are elongated molecules. Based on all current available data along with our photo-cross-linking results using nine single cysteine TnI mutants, a model for TnC and TnI in the Tn complex has been proposed (Luo et al., 2000).

TnT can bind TnI and Tm, and is clearly required to retain TnC and TnI on the thin filament in the Ca^{2+}-free condition. In addition to this structural role, it appears to be involved in elevating the Ca^{2+}-activated ATPase of S1·Tn·Tm·F-actin above that of S1·Tm·F-actin (Farah et al., 1994; Malnic et al., 1998; Oliveira et al., 2000; Potter et al., 1995). This process, usually referred to as activation, involves the N-terminal half of TnI (Van Eyk et al., 1997). An interaction between TnT and TnI attributed to coiled coil formation was first proposed by Pearlstone and Smillie (1985), and has received some experimental support from a recent mutagenesis study using the yeast two-hybrid assay (Stefancsik et al., 1998).

Our early studies on the Ca^{2+}-induced movement of TnI between actin and Tn showed that upon binding of Ca^{2+} to TnC, Cys133 of TnI moves away from actin Cys374 by ~15 Å in the reconstituted Tn·Tm·F-actin thin filament (Tao et al., 1990) and toward TnC Cys98 by ~11.5 Å in the ternary I·C·T Tn complex (Luo et al., 1998; Tao et al., 1989). Our photo-cross-linking study identified TnI Met121 as interacting with TnC's N-domain hydrophobic cleft in the presence of Ca^{2+} and was found to stay in the vicinity of TnC in the absence of Ca^{2+} (Luo et al., 1999a). More recently we showed that whereas TnI residues 104 and 133 interact with actin in the absence of Ca^{2+}, residue 121 does not (Luo et al., 2000). Based on these observations a mechanism was proposed whereby the segment of TnI that contains Met121 (residues 114–125, termed the triggering region) of TnI occupies TnC's N-terminal hydrophobic patch in the presence of Ca^{2+}; in the absence of Ca^{2+} this segment moves out of the patch upon its closing and triggers the movements of the actin binding regions toward actin (Luo et al., 2000).

In this work we further examine the above hypothesis by constructing a mutant rabbit skeletal TnI with a single cysteine at position 117 (I117). Residue 117 was chosen as the mutation site because it immediately follows the inhibitory region and is at the beginning of the less well characterized triggering region (residues 114–125). Knowledge of its location and interactions with the other thin filament proteins will therefore shed much light on the inhibitory function of TnI. The same mutant was constructed and used to assess the flexibility and accessibility of this TnI region and measure the distance between TnI residue 117 and Cys374 of actin (Kobayashi et al., 2000). We conducted a more extended study in which in addition to the distance between this TnI residue and actin Cys374, seven distances between this residue and TnC residues were measured by resonance energy transfer (RET) and used to localize this TnI residue with respect to the crystal structure of TnC. Photo-cross-linking studies using 4-maleimidobenzophnone (BP-Mal)-labeled I117 were also conducted to examine the interactions of this residue with the other thin filament proteins. Our results show that in the presence of Ca^{2+} TnI residue 117 is localized in the vicinity of helices B and C of TnC's N-domain. In the absence of Ca^{2+} it moves away from TnC and toward actin but does not interact with actin. The relevance of these findings to the mechanism whereby the Ca^{2+}-regulatory signal is transmitted from TnC to TnI will be discussed.

MATERIALS AND METHODS

Chemicals

Common reagents were from Sigma (St. Louis, MO). Hepes was from Research Organics (Cleveland, OH), *N*-iodoacetyl-*N*′-(5-sulfo-1-naphthyl) ethylenediamine (1,5-IAEDANS) was from Aldrich (Milwaukee, WI), and BP-Mal, *N*-(4-dimethylamino-3,5-dinitrophenyl)maleimide (DDP-Mal), and 4-dimethylaminophenylazophenyl-4′-maleimide (DAB-Mal) were from Molecular Probes (Eugene, OR). Materials for recombinant DNA procedures were from Life Technologies (Grand Island, NY). The Sequenase kit was from U.S. Biochemicals (Cleveland, OH), and materials for gel electrophoresis were from Bio-Rad (Hercules, CA).

Proteins

Published procedures were used to prepare Tn subunits (Greaser and Gergely, 1973), Tm (Greaser and Gergely, 1971), and actin (Spudich and Watt, 1971) from rabbit skeletal muscle. Mutant I117 cDNA was produced using the polymerase chain reaction method of overlap extension (Ho et al., 1989). Starting from the wild-type rabbit fast skeletal cDNA (Jha et al., 1996) the codons for the three native Cys residues 48, 64, and 133 were replaced with those for Ser. The monocysteine construct was then made by

changing the TCG codon for Ser117, at the C-terminus of the inhibitory region to TGC. Single Cys mutants of TnC were also prepared by procedures described by Wang et al. (1990). The constructs were completely sequenced using the Sequenase kit (U.S. Biochemicals). The expression vector pAED4 and *Escherichia coli* strain BL2 (DE3) were used for expression of the mutant protein as described by Gong et al. (1993).

Labeling of TnC mutants was performed in a medium containing 10 mM Hepes (pH 7.5), 0.1 M NaCl, and 2 mM EDTA. I117 was labeled in a denaturing solution containing 10 mM Hepes (pH 7.5), 4 M guanidinium chloride, 2 mM EDTA, and 0.1 M NaCl. The TnC or TnI solutions, typically 40 μM, were incubated with 5–10 mM dithiothreitol (DTT) for 30 min and dialyzed against the above buffer solutions, but without DTT. This was immediately followed by incubation with 1,5-IAEDANS, DAB-Mal, DDP-Mal, or BP-Mal (120–150 μM) for 3 h at room temperature and then overnight at 4°C. The reactions were quenched with 10 mM DTT, and excess reagents were removed by dialysis. The labeling ratios were determined spectroscopically, using extinction coefficients given in our previous works (Luo et al., 1997; Wang et al., 1992). Typical molar labeling ratios were 0.5 (label:protein) for DAN, >0.8 for DAB and DDP, and 0.8 for BP.

For reconstitution of the binary and ternary complexes, the protein components were mixed stoichiometrically in the denaturing solution described above, then dialyzed against a buffer containing 10 mM Hepes (pH 7.5), 0.1 M NaCl, 50 mM DTT, and 0.2 mM $CaCl_2$. Actin was labeled with 1,5-IAEDANS according to Tao et al. (1983). To reconstitute the Tn·Tm·F-actin-regulated thin filament, the reconstituted Tn complex was mixed with Tm and F-actin to a final molar ratio of 1:1:7 (Tn:Tm:actin). The mixture was then dialyzed against a buffer containing 2 mM Tris, pH 8.0, 50 mM NaCl, 0.2 mM $CaCl_2$, 1 mM $MgCl_2$, 0.2 mM ATP, and 0.5 mM DTT. To change the metal ion conditions from the 4-Ca^{2+} to the 2-Mg^{2+} or apo state, 2 mM EGTA and 8 mM $MgCl_2$ or 2 mM EDTA, respectively, was added to the samples containing 0.2 mM $CaCl_2$.

Fluorescence measurements and data analysis

Fluorescence and anisotropy decay curves were obtained using a modified ORTEC 9200 nanosecond fluorometer as described previously (Tao and Cho, 1979). Fluorescence decay curves were analyzed by the method-of-moments (MOM), using the program FLUOR (Small and Isenberg, 1976) to obtain τ_d and τ_{da}, the donor fluorescence lifetime in the absence and presence of acceptor, respectively. According to Förster's equations (Fairclough and Cantor, 1978), energy transfer efficiency and distance can be calculated as follows:

$$E = 1 - \tau_{da}/\tau_d \quad (1)$$

$$R = R'_o(E^{-1} - 1)^{1/6}, \quad (2)$$

where R_o is the critical transfer distance corrected for the variation in donor fluorescence quantum yield using the equation

$$R_o = R'_o(\tau_{da}/\tau'_d)^{1/6}, \quad (3)$$

with R'_o = 39.9 Å and τ'_d = 13.5 ns as measured previously for the DAN-DAB couple (Tao et al., 1983), and R'_o = 29 Å and τ'_d = 20.6 ns for the DAN-DDP couple (Dalbey et al., 1983).

To determine the position of TnI residue 117 with respect to the framework of the TnC structure, we used a nonlinear least-squares fitting program (Luo et al., 1998), which first computes the calculated distance between the TnI and TnC residues.

$$R_{ic} = \{(x_i - X)^2 + (y_i - Y)^2 + (z_i - Z)^2\}^{1/2}, \quad (4)$$

where x_i, y_i, and z_i are the coordinates of the ith TnC residue's α-carbon in the coordinate system of the TnC crystal structure (Herzberg and James, 1985), and X, Y, and Z are those of TnI residue 117. It then computes the mean squared residual:

$$r^2/N = (1/N)\sum_{i=1}^{n}(R_i - R_{ic})^2, \quad (5)$$

where R_i are the experimental RET-determined distances and N is the number of distances measured. r^2/N is then minimized using X, Y, and Z as variable parameters.

Fluorescence anisotropy decay was measured according to methods described in Tao (1978). The anisotropy $A(t)$ was calculated using the equation:

$$A(t) = [I_{\parallel}(t) - I_{\perp}(t)]/[I_{\parallel}(t) + 2I_{\perp}(t)], \quad (6)$$

where $I_{\parallel}(t)$ and $I_{\perp}(t)$ are the parallel and perpendicular components, respectively, of the polarized emission.

Myofibrillar ATPase measurements

Myofibrils were prepared from rabbit skeletal muscle and depleted of endogenous TnC and TnI as described in detail previously (Luo et al., 1997). Labeled or unlabeled I117, either alone or complexed with labeled or unlabeled TnC mutants, was then added to the extracted myofibrils to final concentrations of 4 μM in proteins and 2 mg/ml in myofibrils and incubated for 5 min at room temperature. The ATPase activity of each preparation was then measured in the absence and presence of Ca^{2+} as described in Luo et al. (1997). The standard errors of the mean (SEM) for the samples containing I·C added back to TnC- and TnI-depleted myofibrils (sample 4 in Fig. 3) were determined to ascertain the typical errors in these measurements. They were 4.4 (3%) and 4.1 (8%) nmol/min-mg in the presence and absence of Ca^{2+}, respectively.

Photo-cross-linking experiments

These were carried out in the same manner as in previous studies (Luo et al., 1997, 2000). $I117^{BP}$·C, $I117^{BP}$·C·T or Tn·Tm·F-actin-containing $I117^{BP}$ in the 4-Ca^{2+}, 2-Mg^{2+}, or apo states (buffer conditions are specified above) were aliquotted (0.3 ml) into borosilicate test tubes. Irradiation was then carried out in a Rayonet RPR-100 photochemical reactor (Southern New England Ultraviolet, Hamden, CT) for 30 min in the cold room (4°C) as described previously (Tao et al., 1985). The photo-cross-linking patterns were analyzed using SDS-polyacrylamide gel electrophoresis (12.5% acrylamide).

RESULTS

This work is divided into four sections. 1) The distance between residue 117 of TnI and residue 98 of TnC, R(I117-C98), was analyzed in detail. 2) The distance between TnI residue 117 and Cys374 of actin, R(I117-A374), was measured. 3) The distances from TnI residue 117 to six additional sites in TnC were measured and incorporated into a distance geometry analysis to localize this residue within the framework of TnC's crystal structure. 4) Photo-cross-linking of BP-Mal-labeled I117 to TnC, TnT, and actin was examined. Native and recombinant rabbit skeletal proteins were used throughout this work.

Distance between TnI residue 117 and TnC residue 98

This was measured using the DAN donor attached at Cys117 of I117 and DDP acceptor attached at Cys98 of native rabbit skeletal TnC, and vice versa. Measurements were made in the binary I·C and ternary I·C·T complexes in three metal-binding states: 1) the 4-Ca^{2+} state (0.2 mM $CaCl_2$) in which all four metal-binding sites in TnC are saturated with Ca^{2+}, simulating the physiological activated state; 2) the 2-Mg^{2+} state (2 mM EGTA, 6 mM $MgCl_2$) in which only the C-terminal high-affinity sites are occupied by Mg^{2+}, simulating the physiological inhibited state; and 3) the apo state (4 mM EDTA), in which none of the sites are occupied.

The methodologies for analyzing the decay curves and for calculating the distances from the decay parameters follow closely those described in Luo et al. (1998). In general, the monoexponential lifetimes of samples containing donor alone is taken as the unquenched lifetime τ_d (Eq. 1; see Materials and Methods), and the shorter of the two biexponential lifetimes of samples containing both donor and acceptor is taken as the quenched lifetime, τ_{da}. Here we briefly illustrate these methods using the data for the ternary I117·C·T complex with the DAN donor on I117 and the DDP acceptor on TnC, measured in the presence of Ca^{2+}. The DAN-DDP donor-acceptor couple was chosen because the distances involved were expected to be closer to its critical transfer distance, $R_o \cong 30$ Å. The fluorescence decay curve of $I117^{DAN}$·C·T (i.e., donor decay in the absence of acceptor) in the presence of Ca^{2+} appears monoexponential by visual inspection (Fig. 1 *A*, *upper curve*). Monoexponential MOM analysis yielded a lifetime, τ, of 16.72 ns (Table 1). Biexponential analysis yielded a major component with a very similar lifetime (16.34 ns) and a minor component with a negligibly small fractional amplitude (0.3%) and a lifetime (54.99 ns) that is too long to be physically meaningful. We conclude that $I117^{DAN}$·C·T decays with a single exponential, as might be expected for a DAN moiety attached at a single site. The monoexponential lifetime of 16.72 ns is therefore taken as τ_d, the unquenched lifetime.

The decay of $I117^{DAN}$·C^{DDP}·T (i.e., donor decay in the presence of acceptor) is clearly multi-exponential (Fig. 1 *A*, *lowest curve*), with a rapid decay at short times that corresponds to donor moieties undergoing energy transfer to acceptor moieties. As expected, monoexponential MOM analysis yielded $\tau = 12.61$ ns, and an extraordinarily large quality-of-fit parameter, χ^2/N (defined in the legend for Table 1), of 21.0. Biexponential MOM analysis of this curve yielded a short- and a long-lived component of $\tau = 9.42$ and 20.89 ns, respectively, with a dramatic decrease in χ^2/N to 4.4. Triexponential analysis yielded a third component of negligibly small fractional amplitude (0.2%) and a physically meaningless lifetime (49.14 ns). We conclude that this

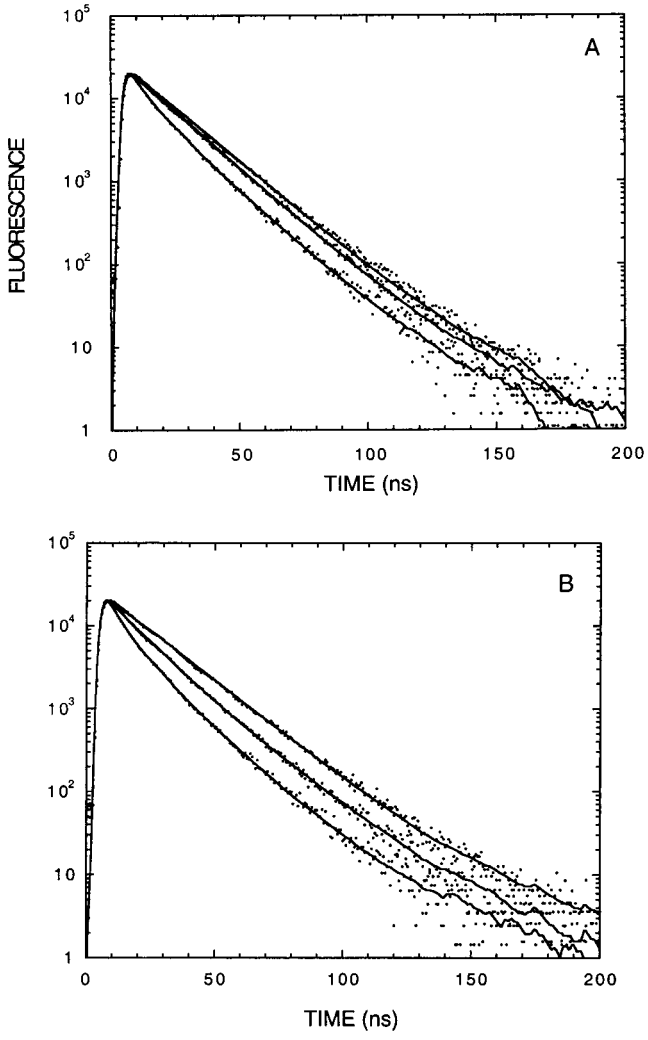

FIGURE 1 Fluorescence decay curves of DAN-labeled I117 ($I117^{DAN}$) in the ternary Tn complex (*A*) and the reconstituted thin filament (*B*). (*A*, *top curve*) $I117^{DAN}$·C·T 4-Ca^{2+}; (*middle curve*) $I117^{DAN}$·C^{DDP}·T, 2-Mg^{2+}; (*bottom curve*) $I117^{DAN}$·C^{DDP}·T, 4-Ca^{2+}. (*B*, *top curve*) $I117^{DAN}$·C·T·Tm·A, 4-Ca^{2+}; (*middle curve*) $I117^{DAN}$· C·T·Tm·A^{DAB}, 4-Ca^{2+}; (*bottom curve*) $I117^{DAN}$·C·T·Tm·A^{DAB}, 2-Mg^{2+}. Dots are experimental points, and solid lines are calculated curves using MOM-derived fluorescence decay parameters (Table 1).

decay is essentially biexponential and that the shorter lifetime can be taken as the quenched lifetime, τ_{da}, in the energy transfer calculations. Substituting the values for τ_d and τ_{da} into the Förster equations (Eqs. 1–3) we obtained a transfer efficiency $E = 43.7\%$, a critical transfer distance $R_o = 28.0$ Å, and separation distance $R = 29.2$ Å (Table 2).

By and large all the decay curves in this study behaved in a similar manner and were therefore analyzed similarly. In general, if biexponential (triexponential) analysis yields a component with a fractional amplitude $<3\%$, then the decay is considered to be monoexponential (biexponential). In some cases, the quenched lifetime is too close to the unquenched lifetime to be resolved by the

TABLE 1 Donor fluorescence decay parameters for RET between DAN-labeled I117 and acceptor-labeled TnC, TnC mutants, and actin

Material	τ_1	(A_1)	τ_2	(A_2)	τ_3	(A_3)	χ^2/N
$I117^{DAN}$, 4-Ca^{2+}	16.95	(1.000)					3.1
	16.77	(0.998)	46.28	(0.002)			2.7
$I117^{DAN}$, 2-Mg^{2+}	16.41	(1.000)					3.7
	16.08	(0.997)	53.71	(0.003)			3.6
$I117^{DAN}$, apo	16.97	(1.000)					3.0
	16.84	(0.999)	60.44	(0.001)			2.7
$I117^{DAN}$·C·T, 4-Ca^{2+}	16.72	(1.000)					6.5
	16.34	(0.997)	54.99	(0.003)			2.7
$I117^{DAN}$·C^{DDP}·T, 4-Ca^{2+}	12.61	(1.000)					21.0
	9.42	(0.852)	20.89	(0.148)			4.4
	6.60	(0.552)	15.32	(0.446)	49.14	(0.002)	2.2
$I117^{DAN}$·C·T, 2-Mg^{2+}	16.95	(1.000)					3.6
	16.90	(1.000)	72.44	(2.4×10^{-4})			3.7
$I117^{DAN}$·C^{DDP}·T, 2-Mg^{2+}	15.65	(1.000)					6.0
	15.16	(0.976)	26.91	(0.024)			5.9
	13.60	(0.723)	19.27	(0.273)	−11.11	(0.003)	—
$I117^{DAN}$·C·T, apo	17.75	(1.000)					5.1
	17.01	(0.984)	39.45	(0.016)			3.1
	16.92	(0.979)	36.93	(0.020)	−28.97	(6.5×10^{-5})	—
$I117^{DAN}$·C^{DDP}·T, apo	14.55	(1.000)					16.6
	11.51	(0.852)	23.26	(0.148)			3.9
	16.65	(0.517)	8.33	(0.480)	51.65	(0.003)	2.4
$I117^{DAN}$·C·T·Tm·A, 4-Ca^{2+}	17.97	(1.000)					4.2
	17.64	(0.997)	56.79	(0.003)			3.6
$I117^{DAN}$·C·T·Tm·A^{DAB}, 4-Ca^{2+}	14.76	(1.000)					9.4
	12.62	(0.887)	23.72	(0.113)			3.7
	11.13	(0.643)	18.21	(0.354)	43.26	(0.003)	3.2
$I117^{DAN}$·C·T·Tm·A, 2·Mg^{2+}	17.83	(1.000)					3.75
	17.51	(0.997)	53.55	(0.003)			3.6
$I117^{DAN}$·C·T·Tm·A^{DAB}, 2-Mg^{2+}	11.20	(1.000)					27.6
	8.24	(0.892)	20.85	(0.108)			6.1
	5.75	(0.646)	14.59	(0.352)	46.20	(0.002)	3.3
$I117^{DAN}$·C·T·Tm·A, apo	17.83	(1.000)					3.6
	17.62	(0.998)	49.97	(0.002)			2.9
$I117^{DAN}$·C·T·Tm·A^{DAB}, apo	12.05	(1.000)					27.4
	7.85	(0.791)	18.73	(0.209)			2.9
	5.72	(0.493)	11.98	(0.409)	20.94	(0.098)	2.3
$I117^{DAN}$·C5·T, 4- Ca^{2+}	17.25	(1.000)					2.9
2	16.73	(0.992)	35.01	(0.008)			1.8
$I117^{DAN}$·$C5^{DDP}$·T, 4-Ca^{2+}	11.54	(1.000)					20.1
	8.04	(0.808)	18.11	(0.192)			2.4
	6.20	(0.601)	14.45	(0.393)	32.45	(0.005)	1.4
$I117^{DAN}$·C5·T, 2·Mg^{2+}	16.73	(1.000)					2.8
	16.26	(0.982)	21.20	(0.018)			1.8
$I117^{DAN}$·$C5^{DDP}$·T, 2-Mg^{2+}	14.32	(1.000)					8.9
	9.69	(0.581)	17.81	(0.419)			1.3
	9.48	(0.566)	17.72	(0.426)	−2.05	(0.008)	—
$I117^{DAN}$·C12·T, 4-Ca^{2+}	17.37	(1.000)					3.0
	16.65	(0.973)	31.37	(0.027)			1.8
$I117^{DAN}$·$C12^{DDP}$·T, 4-Ca^{2+}	12.50	(1.000)					13.5
	7.52	(0.799)	19.97	(0.201)			1.9
	4.69	(0.610)	15.48	(0.386)	40.89	(0.004)	1.3
$I117^{DAN}$·C12·T, 2-Mg^{2+}	16.97	(1.000)					3.2
	16.23	(0.974)	31.44	(0.026)			1.3

(Continued)

TABLE 1 (Continued)

Material	τ_1	(A_1)	τ_2	(A_2)	τ_3	(A_3)	χ^2/N
	16.23	(0.974)	31.44	(0.026)			1.3
$I117^{DAN}$·$C12^{DDP}$·T, 2-Mg^{2+}	14.38	(1.000)					12.3
	9.56	(0.656)	19.01	(0.344)			1.6
	6.52	(0.385)	15.59	(0.592)	27.58	(0.024)	1.3
$I117^{DAN}$·C21·T, 4-Ca^{2+}	17.02	(1.000)					3.6
	16.70	(0.975)	27.41	(0.025)			2.5
$I117^{DAN}$·$C21^{DDP}$·T, 4-Ca^{2+}	12.41	(1.000)					20.3
	7.01	(0.668)	16.91	(0.332)			1.7
	7.22	(0.684)	17.16	(0.316)	50.95	(-6.1×10^{-6})	1.7
$I117^{DAN}$·C21·T, 2-Mg^{2+}	17.00	(1.000)					2.5
	16.79	(0.996)	39.70	(0.004)			2.6
$I117^{DAN}$·$C21^{DDP}$·T, 2-Mg^{2+}	14.95	(1.000)					5.9
	9.26	(0.407)	17.07	(0.593)			1.3
	Complex roots						—
$I117^{DAN}$·C57·T, 4-Ca^{2+}	16.55	(1.000)					8.2
	12.14	(0.968)	33.02	(0.032)			6.5
$I117^{DAN}$·$C57^{DDP}$·T, 4-Ca^{2+}	8.54	(1.000)					44.3
	5.22	(0.926)	19.66	(0.074)			7.8
	2.02	(0.793)	12.11	(0.206)	49.16	(0.001)	7.1
$I117^{DAN}$·C57·T, 2-Mg^{2+}	17.24	(1.000)					9.6
	16.77	(0.983)	31.74	(0.017)			8.5
$I117^{DAN}$·$C57^{DDP}$·T, 2-Mg^{2+}	11.45	(1.000)					39.4
	6.79	(0.765)	17.39	(0.235)			7.2
	5.85	(0.683)	15.62	(0.315)	33.49	(0.003)	7.0
$I117^{DAN}$·C89·T, 4-Ca^{2+}	18.30	(1.000)					2.7
	18.29	(1.000)	253.45	(1.7×10^{-6})			2.6
$I117^{DAN}$·$C89^{DDP}$·T, 4-Ca^{2+}	12.56	(1.000)					15.3
	7.61	(0.767)	19.07	(0.233)			2.5
	6.09	(0.635)	16.11	(0.358)	32.09	(0.008)	2.1
$I117^{DAN}$·C89·T, 2-Mg^{2+}	16.86	(1.000)					3.0
	14.65	(0.978)	21.82	(0.022)			2.0
$I117^{DAN}$·$C89^{DDP}$·T, 2-Mg^{2+}	15.16	(1.000)					6.0
	11.11	(0.606)	18.83	(0.394)			1.5
	12.27	(0.625)	19.45	(0.368)	32.80	(0.007)	1.3
$I117^{DAN}$·C158·T, 4-Ca^{2+}	17.98	(1.000)					2.4
	17.83	(0.998)	51.69	(0.002)			2.1
$I117^{DAN}$·$C158^{DDP}$·T, 4-Ca^{2+}	14.09	(1.000)					23.7
	8.30	(0.684)	19.45	(0.316)			2.2
	5.27	(0.419)	13.91	(0.474)	22.70	(0.107)	1.4
$I117^{DAN}$·C158·T, 2-Mg^{2+}	16.92	(1.000)					3.2
	16.35	(0.980)	31.41	(0.020)			2.5
$I117^{DAN}$·$C158^{DDP}$·T, 2-Mg^{2+}	14.83	(1.000)					9.0
	10.51	(0.640)	19.07	(0.360)			1.1
	10.53	(0.642)	19.09	(0.358)	94.54	(3.3×10^{-8})	1.1

τ_1, τ_2, and τ_3 are lifetimes of decay components. In parentheses are the fractional amplitutes A_1, A_2, and A_3. χ^2/N is the quality-of-fit parameter, defined as $(1/N)\Sigma_{i=1}^{N} (I_{ic} - I_{ie})^2/I_{ie})$ where I_{ic} and I_{ie} are calculated, and experimental intensities for the ith channel, respectively, and N is the number of channels.

MOM program (e.g., $I117^{DAN}$·C^{DDP}·T, 2-Mg^{2+}). The lifetime derived from monoexponential analysis (15.65 ns) was therefore taken as τ_{da}. In other cases nonphysical results such as negative lifetimes (e.g., $I117^{DAN}$·C^{DDP}·T, apo) were obtained. This can be attributed to artifacts arising from the MOM program attempting to analyze a biexponential decay curve with three exponentials. In another instance ($I117^{DAN}$· $C21^{DDP}$· T, 2-Mg^{2+}) the analysis failed, yielding complex roots, presumably for the same reason.

The RET parameters and distances calculated from them are shown in Table 2. It can be seen that R(I117-C98) is largely insensitive to switching of the donor-acceptor locations; the average difference between the two sets of measurements being 9%. The mean of these two distances will be used in further discussion. Second, there is no apparent difference in this distance between the binary and the ternary complexes: 29.4 vs. 30.8 Å in the 4-Ca^{2+} state, 41.8 vs. 40.5 Å in the 2-Mg^{2+} state, and 32.7 vs. 32.7 Å in the apo state. This distance increases by ~10 Å in the 2-Mg^{2+} versus Ca^{2+} state. Finally, the distances measured in the apo state appear to be closer to those measured in the 4-Ca^{2+} than in the 2-Mg^{2+} state.

TABLE 2 Distances from residue 117 of TnI to residues in TnC and actin measured by RET

Material	τ_{da} (ns)	τ_d (ns)	E (%)	R_o (Å)	R (Å)
$I117^{DAN}$·C^{DDP}, 4-Ca^{2+}	8.53	17.97	52.5	28.3	27.9
$I117^{DAN}$·G^{DDP}, 2-Mg^{2+}	15.14	17.21	12.0	28.1	39.2
$I117^{DAN}$·C^{DDP}, apo	11.36	17.68	35.7	28.3	31.2
$I117^{DDP}$·C^{DAN}, 4-Ca^{2+}	11.38	18.19	37.4	28.4	30.9
$I117^{DDP}$·C^{DAN}, 2-Mg^{2+}	15.31	16.23	5.7	27.9	44.5
$I117^{DDP}$·C^{DAN}, apo	13.10	17.15	23.6	28.1	34.2
$I117^{DAN}$·C^{DDP}·T, 4-Ca^{2+}	9.42	16.72	43.7	28.0	29.2
$I117^{DAN}$·C^{DDP}·T, 2-Mg^{2+}	15.65	16.95	7.7	28.0	42.5
$I117^{DAN}$·C^{DDP}·T, apo	11.51	17.75	35.2	28.3	31.3
$I117^{DDP}$·C^{DAN}·T, 4-Ca^{2+}	11.43	18.64	38.7	28.5	30.8
$I117^{DDP}$·C^{DAN}·T, 2-Mg^{2+}	15.27	17.61	13.3	28.2	38.6
$I117^{DDP}$·C^{DAN}·T, apo	13.83	18.38	24.8	28.4	34.2
$I117^{DAN}$·C·T·Tm·A^{DAB}, 4-Ca^{2+}	12.62	17.97	29.8	41.8	48.3
$I117^{DAN}$·C·T·Tm·A^{DAB}, 2-Mg^{2+}	8.24	17.83	53.4	41.8	40.7
$I117^{DAN}$·C·T·Tm·A^{DAB}, apo	7.85	17.83	56.0	41.8	40.1
$I117^{DAN}$·$C5^{DDP}$·T, 4-Ca^{2+}	8.04	17.25	53.4	28.2	27.5
$I117^{DAN}$·$C5^{DDP}$·T, 2-Mg^{2+}	9.69	16.73	42.1	28.0	29.5
$I117^{DAN}$·$C12^{DDP}$·T, 4-Ca^{2+}	7.52	17.37	56.7	28.2	26.9
$I117^{DAN}$·$C12^{DDP}$·T, 2-Mg^{2+}	9.56	16.97	43.7	28.1	29.3
$I117^{DAN}$·$C21^{DDP}$·T, 4-Ca^{2+}	7.01	17.02	58.8	28.1	26.5
$I117^{DAN}$·$C21^{DDP}$·T, 2-Mg^{2+}	9.26	17.00	45.5	28.1	28.9
$I117^{DAN}$·$C57^{DDP}$·T, 4-Ca^{2+}	5.22	16.55	68.5	28.0	24.6
$I117^{DAN}$·$C57^{DDP}$·T, 2-Mg^{2+}	6.79	17.24	60.6	28.1	26.2
$I117^{DAN}$·$C89^{DDP}$·T, 4-Ca^{2+}	7.61	18.30	58.4	28.4	26.9
$I117^{DAN}$·$C89^{DDP}$·T, 2-Mg^{2+}	11.11	16.88	34.2	28.1	31.3
$I117^{DAN}$·$C158^{DAB}$·T, 4-Ca^{2+}	8.30	17.98	53.8	41.8	40.8
$I117^{DAN}$·$C158^{DAB}$·T, 2-Mg^{2+}	10.51	16.92	37.9	41.4	45.0

τ_d and τ_{da} are donor lifetimes in the absence and presence of acceptor, respectively, used in the calculation of E, the energy transfer efficiency (Eq. 1). R_o is the critical transfer distance (Eq. 3); R is the separation distance (Eq. 2).

Polarization results

Some of the samples that were used for measuring R(I117-C98) were subjected to polarization anisotropy decay measurements. The anisotropy, $A(t)$, of uncomplexed $I117^{DAN}$ decays rapidly (Fig. 2), as expected for a freely rotating protein of $M_r = 21{,}000$. It is not Ca^{2+} dependent, also expected because free TnI does not bind divalent metal ions. $A(t)$ for $I117^{DAN}$·C·T decays more slowly owing to the larger molecular volume of the ternary Tn complex. Rapid $A(t)$ decay components that might indicate dissociation of the complex are absent. $A(t)$ is not Ca^{2+} dependent, indicating that there is no significant dissociation of the complex upon removal of Ca^{2+} from the N-domain sites of TnC. $A(t)$ curves for $I117^{DAN}$·C^{DDP}·T are similar to those of $I117^{DAN}$·C·T, indicating that the presence of both probes in the complex did not induce dissociation of the complexes. As for the singly labeled complexes, $A(t)$ of the doubly labeled complexes are not Ca^{2+} dependent. Only for $I117^{DAN}$·C and $I117^{DAN}$·C^{DDP} in the apo state are the $A(t)$ decay rates (data not shown) significantly increased, indicating that there might be some complex dissociation. It should be noted that because lifetime measurements were carried out here, slight dissociation affects only the amplitude of the quenched component and not its lifetime. Thus, dissociation should have only small effects on the distance determinations.

The values of the anisotropy at zero time, A_o, were determined from the anisotropy decay curves to be 0.159, 0.195, 0.187, 0.199, and 0.205 (averages of the values measured in the presence and absence of Ca^{2+}) for $I117^{DAN}$, $I117^{DAN}$·C, $I117^{DAN}$·C·T, $I117^{DAN}$· C^{DDP}, and $I117^{DAN}$·C^{DDP}·T, respectively.

Regulatory properties of the complexes

The capacity of the I117·C complex containing labeled and unlabeled proteins to regulate myofibrillar ATPase activity was evaluated using the procedure described in Materials and Methods. As shown in Fig. 3, intact myofibrils (i.e., myofibrils before extraction) exhibit normal regulatory behavior. Myofibrils extracted of TnI and TnC are unregulated; the preparation is active both in the presence and absence of Ca^{2+}. As expected, addition of native rabbit skeletal TnI to the extracted myofibrils inhibited the ATPase both in the presence and absence of Ca^{2+}. Addition of TnI together with native TnC largely restored the regulatory activity. This set of experiments serves as the controls for this procedure. Addition of I117, $I117^{DAN}$, and $I117^{DDP}$ produced the same result as that of native TnI, indicating that neither the mutation nor the labeling affected the ability of TnI to interact with actin and inhibit actomyosin ATPase. Addition of I117, $I117^{DAN}$, and $I117^{DDP}$ together with na-

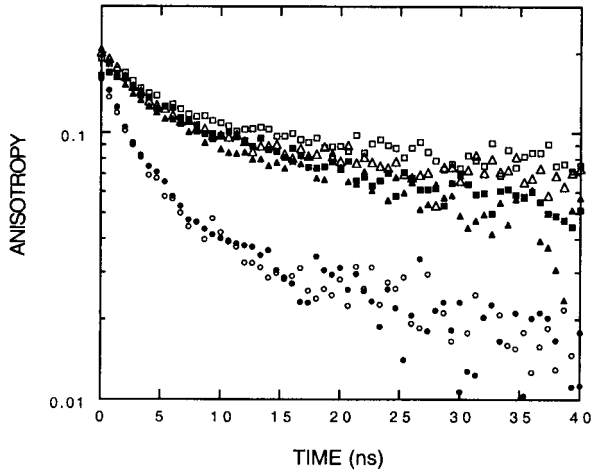

FIGURE 2 Anisotropy decay of $I117^{DAN}$. ● and ○, $I117^{DAN}$, 4-Ca^{2+} and 2-Mg^{2+}, respectively; ■ and □, $I117^{DAN}$·C·T, 4-Ca^{2+} and 2-Mg^{2+}, respectively; ▲ and △, I^{DAN}·C^{DDP}·T, 4-Ca^{2+} and 2-Mg^{2+}, respectively. Measurements were made at protein concentrations of ~4 μM in TnI and temperature of 25°C. There is no rapid initial decay in the curves for the ternary Tn complexes, indicating no substantial dissociation.

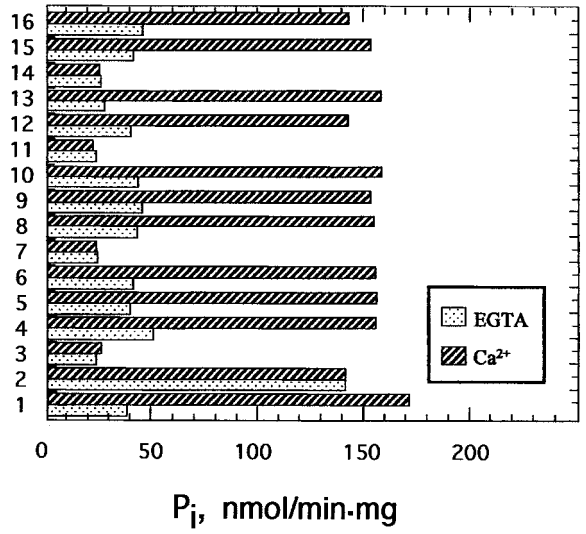

FIGURE 3 Regulatory properties of I117, $I117^{DAN}$, and $I117^{DPP}$. Myofibrillar ATPase measurements (amounts of inorganic phosphate liberated) were done at 22°C, in the presence of EGTA (*dotted bars*) or Ca^{2+} (*hatched bars*). Bars are numbered as follows: 1, control untreated myofibrils; 2, myofibrils extracted of TnC and TnI; all the other bars refer to extracted myofibrils with the following additions: 3, TnI; 4, I·C; 5, I·C^{DAN}; 6, I·C^{DDP}; 7, I117; 8, I117·C; 9, $I117C^{DAN}$; 10, I117·C^{DDP}; 11, $I117^{DAN}$; 12, $I117^{DAN}$·C; 13, $I117^{DAN}$·C^{DDP}; 14, $I117^{DDP}$; 15, $I117^{DDP}$·C; 16, 117^{DDP}·C^{DAN}.

tive TnC restored the regulatory activity to the same extent as that of re-added native TnI and TnC, indicating that the mutated and labeled TnI retained their capacity to regulate myofibrillar ATPase. Addition of native TnI together with C^{DAN} or C^{DDP} also restored the regulatory activity, indicating that labeling of TnC has no effect on its function. Finally, addition of $I117^{DAN}$ together with C^{DDP} or of $I117^{DDP}$ together with C^{DAN} resulted in normal regulatory properties, indicating that the doubly labeled complexes also retain their regulatory functions. We conclude that neither the mutations nor the modifications on TnI or TnC have any drastic effect on their capacities to regulate myofibrillar ATPase activity at maximal and minimal Ca^{2+} concentrations. However, small structural and functional perturbations in the labeled and unlabeled mutants, especially in the absence of Ca^{2+}, cannot be ruled out.

Distance between residues 117 of TnI and Cys374 of actin

R(I117-A374) was measured with the DAN donor on I117 and the DAB acceptor on actin. This donor-acceptor pair was chosen because the distances can be expected to be closer to its R_o value of ~40 Å. Considerable quenching was observed in both the 4-Ca^{2+} and the 2-Mg^{2+} state (Fig. 1 *B*). In this case more quenching was observed in the absence than in the presence of Ca^{2+}, indicating that the DAN donor moves closer to the DAB acceptor in the 2-Mg^{2+} state. Analysis of the decay curves (Table 1) and application of the Förster equations yielded an interprobe distance of 49 Å in the 4-Ca^{2+} state, which decreases by ~8 Å in the 2-Mg^{2+} state (Table 2). The distance measured in the apo state is similar to that measured in the 2-Mg^{2+} state.

Localization of TnI residue 117 relative to the crystal structure of TnC

In addition to *R*(I117-C98), six additional distances from TnI residue 117 to TnC residues 5, 12, 21, 57, 89, and 158 in the ternary Tn complexes were measured. They were used to determine the position of TnI residue 117 relative to the atomic coordinates of TnC derived from its crystal structure. Considering that *R*(I117-C98) is invariant with donor-acceptor locations, these distances were measured only with the donor on I117. A nonlinear least-squares program was then used to determine the position of TnI residue 117 that minimizes the residuals between the measured and calculated distances, assuming that TnC in the ternary complex adopts the same structure as its crystal structure (Luo et al., 1998). In this determination, *R*(I117-C98) was taken to be the average of the two distances measured in the ternary complex. Also, although the coordinates for the crystal structure of TnC in the fully Ca^{2+}-saturated state are now available (Houdusse et al., 1997; Soman et al., 1999), we continued to use the coordinates derived from the molecular modeling studies (Herzberg et al., 1986) to facilitate comparisons with our previous work on the localization of TnI residue 133. This seems justified

because the model structure differs only slightly from the determined crystal structures. The results show that in the 4-Ca^{2+} state TnI's residue 117 is localized near the B-C linker on the B-helix side (Table 3 and Fig. 4). When the determination was repeated in the absence of Ca^{2+} this position moved 8.1 Å away from that determined in the presence of Ca^{2+} (Fig. 4).

Photo-cross-linking studies

Photo-cross-linking of $I117^{BP}$ in the binary I·T, binary I·C, ternary I·C·T complexes, and reconstituted Tn·Tm·F-actin thin filament were examined. In I·C, two photo-cross-linking bands were observed in the 4-Ca^{2+} state, indicating that cross-linking occurred at two locations in TnC (Fig. 5). Only one band was observed in the 2-Mg^{2+} and apo states. In I·T, a single band with an electrophoretic mobility consistent with the molecular mass of a TnI-TnT photo-cross-linking product was observed (data not shown). In I·C·T, the band corresponding to TnI-TnT cross-linking is absent, whereas the same TnI-TnC photo-cross-linking bands as those in I·C were observed (Fig. 5). The most striking observation is that in Tn·Tm·F-actin no photo-cross-linking band that might correspond to TnI-actin cross-linking was observed, suggesting that TnI residue 117 does not interact with actin in the 2-Mg^{2+} or any other state.

DISCUSSION

Orientation factor

The Förster equations contain the orientation factor κ^2, the only quantity that cannot be determined experimentally. We have assumed here that κ^2 takes on the isotropically averaged value of 2/3, the validity of which was examined for the case of *R*(I117-C98). We first consider the fact that the zero time anisotropy, A_o, for $I117^{DAN}$ in all its complexation forms ranges from 0.187 to 0.205, considerably smaller than the maximum value of 0.4 for the case of completely immobilized rotors. This indicates that the orientation of the DAN moiety's transition moment is substantially randomized within the lifetime of the fluorescence, a condition that supports our assumption of $\kappa^2 = 2/3$. Secondly, Stryer (1978) pointed out that one method to check whether the assumption of $\kappa^2 = 2/3$ is valid is to determine whether a measured distance is unchanged when the positions of the donor and the acceptor are switched. In this work *R*(I117-C98) was measured in I·C and I·C·T, each in the three metal-binding states first with the donor on I117 and acceptor on TnC, then with the probe locations switched. The differences in the measured distance with switching of donor-acceptor locations range from 1.6 to 5.3 Å, with a mean of 3.3 Å (Table 2). We conclude that *R*(I117-C98) is essentially invariant with donor-acceptor location, in support of our assumption of $\kappa^2 = 2/3$. In all of our previous studies, neither switching of the donor-acceptor locations nor changing the acceptor had any appreciable effect on the value of the measured distances (see, e.g., Luo, et al., 1998) indicating that the assumption of $\kappa^2 = 2/3$ may be valid in all our studies. This may be an intrinsic property of the particular donor (DAN) and acceptors (DDP and DAB) that we use or due to the fact that most protein side chains to which the probes are attached have sufficient thermal motion to randomize the mutual orientations of the probes

TABLE 3 Comparison of measured and calculated distances between TnI residue 117 and residues in TnC

	4-Ca^{2+}		2-Mg^{2+}	
Residue	Measured	Calculated	Measured	Calculated
5	27.50	34.11	35.20	36.78
12	26.90	29.59	29.30	34.06
21	26.50	20.16	28.90	23.91
57	24.60	23.78	26.20	24.51
89	26.90	22.94	31.30	29.18
98	30.00	30.97	40.50	38.41
158	40.80	40.01	43.60	46.61

For fitted 4-Ca^{2+}, $X, Y, Z = 25.34, 31.02, -21.28$; $r^2/N = 15.58$. For fitted 2-Mg^{2+}, $X, Y, Z = 23.58, 35.93, -27.46$; $r^2/N = 10.12$.
r^2/N is defined in Eq. 5.

Properties of *R*(I117-C98)

This distance is similar in I·C and I·C·T (29.4 vs. 30.0, 41.8 vs. 40.5, and 32.7 vs. 32.7 Å in the 4-Ca^{2+}, 2-Mg^{2+}, and apo states, respectively). This seems to be at variance with our previous studies showing that the conformations of TnI and TnC are altered by the presence of TnT in the Tn complex (Luo et al., 1997; Tao et al., 1999). It has been proposed that TnT interacts with residues 34–89 in the C-terminal portion of TnI via coiled coil interaction (Pearlstone and Smillie, 1985; Stefancsik et al., 1998), and we have proposed that this induces a conformation change that extends this TnI segment away from TnC's C-terminal domain (Luo et al., 2000). However, in this study (see below) and in our previous study (Luo et al., 1999b), both of which use intact proteins, we have evidence that the region comprising TnI residue 117 interacts with TnC's N-terminal domain and is relatively far from the putative TnT interaction site. Thus our finding that TnT has no effect on *R*(I117-C98) suggests that in the ternary Tn complex TnT interacts only with the N- and not the C-terminal portion of TnI.

It is interesting that *R*(I117-C98) measured in the apo state is different from that in the 2-Mg^{2+} state, and closer to that in the 4-Ca^{2+} state. The increase in *R*(I117-C98) in going from the 4-Ca^{2+} to the 2-Mg^{2+} state is attributable to the movement of the TnI residue 117 region away from TnC upon the removal of Ca^{2+} from the metal-binding sites and the closing of the hydrophobic cleft in TnC's N-domain cleft. Cys98 in TnC's C-domain is presumed not to move

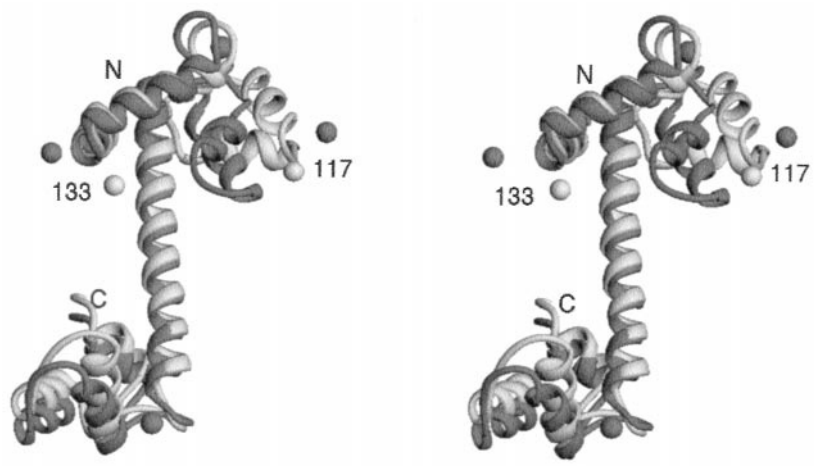

FIGURE 4 Stereo view of the positions of TnI residues 117 and 133 relative to TnC's crystal structure. The positions of the residues are marked by spheres. The shading of the spheres and of the TnC polypeptide chains indicates the two states: light, 4-Ca^{2+} state; dark, 2-Mg^{2+} state. The termini of the chains are marked by N and C. TnI residues 133 and 117 are located near TnC's N-A and B-C helices in the N-terminal domain, respectively. Both move away from TnC in the absence of Ca^{2+}, but in different directions.

because the C-domain metal-binding sites are occupied in both states. Going from the 2-Mg^{2+} to the apo state is not likely to affect the movements of TnI residue 117 because it is localized near TnC's N-domain (see below) and TnC's N-domain sites are unoccupied in both states. However, because the C-domain sites are occupied by Mg^{2+} in the 2-Mg^{2+} state and unoccupied in the apo state, this transition may affect the conformation of TnC's C-domain. Our finding here may be a reflection of this conformational transition. It is known that the C-domain for free TnC is unfolded in the apo state (Leavis et al., 1978). In the I·C and I·C·T, it may be presumed that the presence of TnI and both TnI and TnT maintains the conformation of TnC's C-domain even when the C-domain sites are unoccupied. Our results here indicate that this is not so, or at least that the conformation of TnC's C-domain is different in the 2-Mg^{2+} versus the apo state even in the I·C and I·C·T complexes. The significance of the finding that *R*(I117-C98) in the apo state is similar to that in the 4-Ca^{2+} state is not clear. It may be that the movement of TnC Cys98 compensates for the movement of TnI residue 117, so that the similarity in this distance between the two states is fortuitous.

R(I117-C98) may be compared to *R*(I133-C98), which was originally measured by Tao et al. (1989) using the DAN-DAB donor acceptor pair and was recently remeasured using the more appropriate DAN-DDP pair (Luo et al., 1998). In both cases the measurements were made with the donor on TnC Cys98 and the acceptor on TnI Cys133, and vice versa. The latter study found *R*(I133-C98) to be 29.0 vs. 30.1 Å in the binary versus the ternary complex in the Ca^{2+} state, and 40.5 vs. 45.2 Å in the 2-Mg^{2+} state. It appears that in the Tn complex residues 117 and 133 of TnI are roughly equidistant from Cys98 of TnC.

Properties of *R*(I117-A374)

We found this distance to be 48.3 Å in the 4-Ca^{2+} state and 40.7 Å in the 2-Mg^{2+} state, indicating that TnI residue 117 moves toward actin Cys374 by ~8 Å upon the removal of Ca^{2+}. In comparison, TnI Cys133 moves toward the same actin residue by 15 Å, nearly twice as much.

This distance was also measured by Kobayashi et al. (2000), who reported it to be 43.3 and. 35.2 Å in the presence versus the absence of Ca^{2+}, respectively, ~5 Å shorter than our values. The origin of this difference is not clear, but it may be due to the fact that we used time decay measurements analyzed with discrete distances, whereas

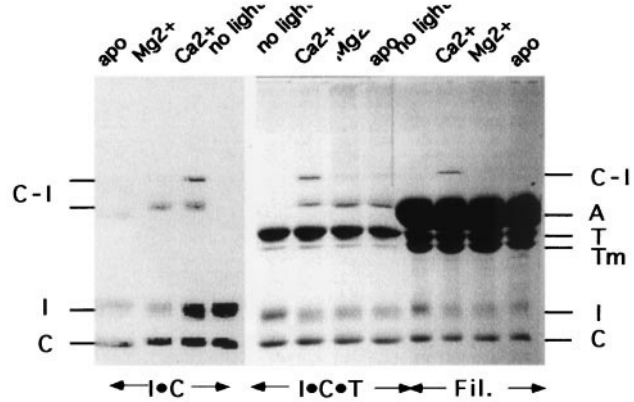

FIGURE 5 Photo-cross-linking of $I117^{BP}$ in the I·C binary, the ternary, and the Tn·Tm·F-actin thin filament complexes. Gels (12.5%) were stained with Coomassie Blue. A, actin; C, TnC; I, TnI; T, TnT; C-I, TnC-TnI photo-cross-linked products; Fil., reconstituted thin filament. Samples (~6 μM in TnI) were irradiated for 30 min in the cold room (4°C). $I117^{BP}$ photo-cross-links only to TnC in I·C·T, and does not photo-cross-link to actin in Tn·Tm·F-actin.

Kobayashi et al. (2000) used phase-modulation measurements analyzed with distance distributions. However, with respect to the decrease in this distance by ~8 Å upon the removal of Ca^{2+} the two studies are in excellent agreement.

Localization of TnI residue 117 with respect to the crystal structure of TnC

Our results show that in the Tn complex and the presence of Ca^{2+} TnI residue 117 is localized in the vicinity of helices B and C of TnC's N-domain (Fig. 4). For comparison, our previous study has localized TnI residue 133 close to helices N and A of TnC's N-domain (Luo et al., 1998). These locations are such that the two residues are indeed roughly equidistant from TnC's Cys98 (see above). That the segment containing TnI residue 117 interacts with this region of TnC's N-domain, more specifically, TnC's N-domain cleft, was proposed by Vassylyev et al. (1998) based on sequence similarities. NMR studies concluded that peptides containing residues 117–121 bind to TnC's N-domain cleft. Our study on the I·C·T complex has shown that a BP probe placed at either TnC residue 48 (in the B-C linker) or 82 (in the D-helix) photo-cross-linked to TnI residue 121, four residues away from residue 117 (Luo et al., 1999a). It provided the first concrete evidence that this TnI region interacts with TnC's N-domain cleft in the intact Tn complex. The fact that this present study, using the completely independent technique of RET, localizes residue 117 in the same general region of TnC provides added confidence in our conclusions. However, the location of residue 117 in the present work appears to be outside the TnC's N-domain cleft, which may seem inconsistent with the findings cited above. It is possible, however, that in this particular case the bulky probe attached at this residue cannot be accommodated within the cleft when the interactions between these regions of TnI and TnC take place.

In the 2-Mg^{2+} state, TnI residue 117 is found 8 Å away from its position in 4-Ca^{2+} state, presumably in response to the closing of TnC's N-domain cleft. Thus, as in the case of TnI residue 133, residue 117 moves away from TnC and toward actin upon the removal of Ca^{2+}. However, as will be discussed below, it appears not to interact with actin in this state.

Residue 117 of TnI photo-cross-links to TnC but not actin

Our results showing that $I117^{BP}$ photo-cross-linked to TnT in I·T and not in I·C·T indicates that the interaction between TnT and the residue 117 region of TnI region is not the same in the two complexes. It is possible that relatively weak TnI-TnT interactions can occur in the binary complex, but stronger TnI-TnC interactions become preferential in the ternary complex. In contrast, the photo-cross-linking patterns between $I117^{BP}$ and TnC are identical in I·C and I·C·T under all three metal-binding conditions, indicating that TnT has no effect on the TnI-TnC interaction, and most likely does not interact with either TnI or TnC in this region of the Tn complex (see also section on properties of *R*(I117-C98) above).

The photo-cross-linking between $I117^{BP}$ and TnC in the 4-Ca^{2+} state is characterized by two distinct bands that most likely correspond to photo-cross-linking to two sites in TnC that are well separated in the primary structure. This observation well complements our previous observation that $I121^{BP}$ also photo-cross-links to TnC at two sites under the same condition (Luo et al., 2000). If TnI residues 117 and 121 are indeed within TnC's N-terminal hydrophobic pocket then these two sites are likely to be in TnC's helix B and helix D. Unlike $I121^{BP}$, however, $I117^{BP}$ photo-cross-links to TnC at only one site in the 2-Mg^{2+} and apo states. It appears that the BP probe attached at residue 117 moves well away from one but not the other TnC site upon the closing of TnC's N-terminal cleft. Which one is which is difficult to ascertain, but if Fig. 4 can be used as a guide, then the B-helix is more likely to be the region that remains close to the BP probe in the 2-Mg^{2+} state.

It is noteworthy that when we used the same methodology as in our previous studies (Luo et al., 1999a, 2000), $I117^{BP}$ does not photo-cross-link to actin in the complete Tn·Tm·F-actin synthetic thin filament under any metal-binding condition. This is in contrast to $I104^{BP}$ and $I133^{BP}$, both of which strongly photo-cross-linked to actin in the 2-Mg^{2+} state (Luo et al., 2000). It could be argued that no photo-cross-linking was observed because the BP probe attached at residue 117 is fortuitously oriented away from actin even though the region containing this residue is in the proximity of actin sites. We believe this to be unlikely because the BP probe is attached to the sulfhydryl group of Cys117 via the maleimido group and has two bonds about which free rotation can take place. Also, we have found that BP attached at TnI residue 121 does not photo-cross-link to actin under the same conditions (Luo et al., 2000). Taken together, it seems more likely that the entire region containing both residues 117 and 121 interacts only with TnC and not with actin.

CONCLUSIONS

In conclusion, our findings here indicate that in the ternary Tn complex residue 117 of TnI is located near the B-C linker region of TnC and that it moves ~8 Å away from this location when Ca^{2+} is removed. In the thin filament, upon the removal of Ca^{2+}, residue 117 moves ~8 Å toward Cys374 of actin but does not appear to make contact with actin. These findings provide independent experimental support for the following scenario that we have proposed in previous reports (Luo et al., 1999a, 2000): in the 4-Ca^{2+} state, TnI's triggering region (residues 114–125), contain-

ing residues 117 and 121, interacts strongly with the open N-terminal hydrophobic cleft of TnC, holding the two actin-binding regions, residues 89–113 and 130–150, away from actin. Upon the removal of Ca^{2+}, the triggering region moves out of TnC's N-domain cleft upon the latter's closing but remains close to TnC and does not itself interact with actin. Nevertheless, it triggers a conformational change in TnI that initiates the movements of the two actin-binding regions toward actin.

We thank Drs. Z. Grabarek and Y. Luo for critically reviewing the manuscript and many helpful discussions. We thank Dr. K. Langsetmo for assistance in preparing some of the figures.

This work was supported by a grant from the National Institutes of Health, AR21673.

REFERENCES

Dalbey, R. E., J. Weiel, and R. G. Yount. 1983. Förster energy transfer measurements of thiol 1 to thiol 2 distances in myosin subfragment 1. *Biochemistry.* 22:4696–4706.

Fairclough, R. H., and C. R. Cantor. 1978. The use of singlet-singlet transfer to study macromolecular assemblies. *Methods Enzymol.* 28: 347–379.

Farah, C. S., C. A. Miyamoto, C. H. I. Ramos, A. C. R. da Silva, R. B. Quaggio, K. Fujimori, L. B. Smillie, and F. C. Reinach. 1994. Structural and regulatory functions of the NH_2- and COOH-terminal regions of skeletal muscle troponin I. *J. Biol. Chem.* 269:5230–5240.

Farah, C. S., and F. C. Reinach. 1995. The troponin complex and regulation of muscle contraction. *FASEB J.* 9:755–767.

Fujimori, K., M. Sorenson, O. Herzberg, J. Moult, and F. C. Reinach. 1990. Probing the calcium-induced conformational transition of troponin-C with site-directed mutants. *Nature.* 345:182–184.

Gagne, S. M., S. Tsuda, M. X. Li, L. B. Smillie, and B. D. Sykes. 1995 Structures of the troponin C regulatory domains in the apo and calcium-saturated states. *Nat. Struct. Biol.* 2:784–789.

Gong, B.-J., K. Mabuchi, K. Takahashi, B. Nadal-Ginard, and T. Tao. 1993. Characterization of wild type and mutant chicken gizzard αcalponin expressed in *E. coli. J. Biochem.* 114:453–456.

Gordon, A. M., E. Homsher, and M. Regnier. 2000. Regulation of contraction in striated muscle. *Physiol. Rev.* 80:853–924.

Grabarek, Z., W. Drabikowski, P. C. Leavis, S. S. Rosenfeld, and J. Gergely. 1981. Proteolytic fragments of troponin C: interactions with the other troponin subunits and biological activity. *J. Biol. Chem.* 256: 13121–13127.

Grabarek, Z., R.-Y. Tan, J. Wang, T. Tao, and J. Gergely. 1990. Inhibition of mutant troponin C activity by an intra-domain disulphide bond. *Nature.* 345:132–135.

Grabarek, Z., T. Tao, and J. Gergely. 1992. Molecular mechanism of troponin-C function. *J. Muscle Res. Cell Motil.* 13:383–393.

Greaser, M. L., and J. Gergely. 1971. Reconstitution of Tn activity from three protein components. *J. Biol. Chem.* 246:4226–4233.

Greaser, M. L., and J. Gergely. 1973. Purification and properties of the components from troponin. *J. Biol. Chem.* 248:2125–2133.

Herzberg, O., and M. N. G. James. 1985. Structure of the calcium regulatory muscle protein troponin-C at 2.8 Å resolution. *Nature.* 313: 653–659.

Herzberg, O., J. Moult, and M. N. G. James. 1986. A model for the Ca^{2+}-induced conformational transition of troponin C. *J. Biol. Chem.* 261:2638–2644.

Ho, S. N., H. D. Hunt, R. M. Horton, J. K. Pullen, and L. R. Pease. 1989. Site-directed mutagenesis by overlap extension using the polymerase chain reaction. *Gene.* 77:51–59.

Houdusse, A., M. L. Love, R. Dominguez, Z. Grabarek, and C. Cohen. 1997. Structures of four Ca^{2+}-bound troponin C at 2.0 Å resolution: further insights into the Ca^{2+}-switch in the calmodulin superfamily. *Structure.* 5:1695–1711.

Jha, P. K., C. Mao, and S. Sarkar. 1996. Photo-cross-linking of rabbit skeletal troponin I deletion mutants with troponin C and its thiol mutants: the inhibitory region enhances binding of troponin I fragments to troponin C. *Biochemistry.* 35:11026–11035.

Kobayashi, T., M. Kobayashi, Z. Gryczynski, J. R. Lakowicz, and J. H. Collins. 2000. Inhibitory region of troponin I: Ca^{2+}-dependent structural and environmental changes in the troponin-tropomyosin complex and in reconstituted thin filaments. *Biochemistry.* 39:86–91.

Kobayashi, T., T. Tao, J. Gergely, and J. H. Collins. 1994. Structure of the troponin complex. Implications of photocross-linking of troponin I to troponin C thiol mutants. *J. Biol. Chem.* 269:5725–5729.

Kobayashi, T., T. Tao, Z. Grabarek, J. Gergely, and J. H. Collins. 1991. Cross-linking of residue 57 in the regulatory domain of a mutant rabbit skeletal muscle troponin C to the inhibitory region of troponin I. *J. Biol. Chem.* 266:13746–13751.

Krudy, G. A., Q. Kleerekoper, X. D. Guo, J. W. Howarth, R. J. Solaro, and P. R. Rosevear. 1994. NMR studies delineating spatial relationships within the cardiac troponin I-troponin C complex. *J. Biol. Chem.* 269: 23731–23735.

Leavis, P. C., and J. Gergely. 1984. Thin filament proteins and thin filament-linked regulation of vertebrate muscle contraction. *CRC Crit. Rev. Biochem.* 16:235–305.

Leavis, P. C., S. Rosenfeld, and R. C. Lu. 1978. Cleavage of a specific bond in troponin C by thrombin. *Biochim. Biophys. Acta.* 535:281–286.

Leszyk, J., J. H. Collins, P. C. Leavis, and T. Tao. 1987. Cross-linking of rabbit skeletal muscle troponin with the photoactive reagent 4-maleimidobenzophenone: identification of residues in troponin I that are close to cysteine-98 of troponin C. *Biochemistry.* 26:7042–7047.

Leszyk, J., J. H. Collins, P. C. Leavis, and T. Tao. 1988. Cross-linking of rabbit skeletal muscle troponin subunits: labeling of cysteine-98 of troponin C with 4-maleimidobenzophenone and analysis of products formed in the binary complex with troponin I and the ternary complex with troponins I and T. *Biochemistry.* 27:6983–6987.

Leszyk, J., Z. Grabarek, J. Gergely, and J. H. Collins. 1990. Characterization of zero length cross-links between rabbit skeletal muscle troponin C and troponin I: evidence for direct interaction between the inhibitory region of troponin I and the NH_2-terminal regulatory domain of troponin C. *Biochemistry.* 29:299–304.

Li, M. X., L. Spyracopoulos, and B. D. Sykes. 1999. Binding of cardiac troponin-I147–163 induces a structural opening in human cardiac tropoin-C. *Biochemistry.* 38:8289–8298.

Luo, Y., J. Leszyk, Y. Qian, J. Gergely, and T. Tao. 1999a. Residues 48 and 82 at the N-terminal hydrophobic patch of troponin-C photo-cross-link to Met121 of troponin-I. *Biochemistry.* 38:6678–6688.

Luo, Y., B. Li, J. Gergely, and T. Tao. 1999b. Interactions of troponin-I Met121 with the N-terminal hydrophobic pocket of troponin-C. *Biophys. J.* 76:A158.

Luo, Y., J.-L. Wu, J. Gergely, and T. Tao. 1997. Troponin T and Ca^{2+} dependence of the distance between Cys48 and Cys133 of troponin I in the ternary troponin complex and reconstituted thin filaments. *Biochemistry.* 36:11027–11035.

Luo, Y., J.-L. Wu, J. Gergely, and T. Tao. 1998. Localization of Cys133 of rabbit skeletal troponin-I with respect to troponin-C by resonance energy transfer. *Biophys. J.* 74:3111–3119.

Luo, Y., J. L. Wu, B. Li, K. Langsetmo, J. Gergely, and T. Tao. 2000. Photo-cross-linking of benzophenone-labeled single cysteine troponin I mutants to other thin filament proteins. *J. Mol. Biol.* 296:899–910.

Malnic, B., C. S. Farah, and F. C. Reinach. 1998. Regulatory properties of the NH_2- and COOH-terminal domains of troponin T. ATPase activation and binding to troponin I and troponin C. *J. Biol. Chem.* 273: 10594–10601.

McKay, R. T., J. R. Pearlstone, D. C. Corson, S. M. Gagne, L. B. Smillie, and B. D. Sykes. 1998. Structure and interaction site of the regulatory domain of troponin-C when complexed with the 96–148 region of troponin-I. *Biochemistry.* 37:12419–12430.

McKay, R. T., B. P. Tripet, R. S. Hodges, and B. D. Sykes. 1997. Interaction of the second binding region of troponin I with the regulatory domain of skeletal muscle troponin C as determined by NMR spectroscopy. *J. Biol. Chem.* 272:28494–28500.

McKay, R. T., B. P. Tripet, J. R. Pearlstone, L. B. Smillie, and B. D. Sykes. 1999. Defining the region of troponin-I that binds to troponin-C. *Biochemistry.* 38:5478–5489.

Olah, G. A., S. E. Rokop, C.-L. A. Wang, S. L. Blechner, and J. Twewhella. 1994. Troponin I encompasses an extended troponin C in the Ca^{2+}-bound complex: a small-angle x-ray and neutron scattering study. *Biochemistry.* 33:8233–8239.

Oliveira, D. M., C. R. Nakaie, A. D. Sousa, C. S. Farah, and F. C. Reinach. 2000. Mapping the domain of troponin T responsible for the activation of actomyosin ATPase activity: identification of residues involved in binding to actin. *J. Biol. Chem.* 275:27513–27519.

Pearlstone, J. R., and L. B. Smillie. 1985. The interaction of rabbit skeletal muscle troponin-T fragments with troponin-I. *Can. J. Biochem. Cell. Biol.* 63:212–218.

Pearlstone, J. R., and L. B. Smillie. 1995. Evidence for two-site binding of troponin I inhibitory peptides to the N and C domains of troponin C. *Biochemistry.* 34:6932–6940.

Pearlstone, J. R., B. D. Sykes, and L. B. Smillie. 1997. Interactions of structural C and regulatory N domains of troponin C with repeated sequence motifs in troponin I. *Biochemistry.* 36:7601–7606.

Perry, S. V. 1998. Troponin T: genetics, properties and function. *J. Muscle Res. Cell Motil.* 19:575–602.

Perry, S. V. 1999. Troponin I: inhibitor or facilitator. *Mol. Cell. Biochem.* 1999:9–32.

Potter, J. D., Z. Sheng, B. S. Pan, and J. Zhao. 1995. A direct regulatory role for troponin T and a dual role for troponin C in the Ca^{2+} regulation of muscle contraction. *J. Biol. Chem.* 270:2557–2562.

Sheng, Z., B. S. Pan, T. E. Miller, and J. D. Potter. 1992. Isolation, expression, and mutation of a rabbit skeletal muscle cDNA clone for troponin I. The role of the NH_2 terminus of fast skeletal muscle troponin I in its biological activity. *J. Biol. Chem.* 267:25407–25413.

Slupsky, C. M., and B. D. Sykes. 1995. NMR solution structure of calcium-saturated skeletal muscle troponin C. *Biochemistry.* 34: 15953–15964.

Small, E. W., and I. Isenberg. 1976. The use of moment index displacement in analyzing fluorescence time-decay data. *Biopolymers.* 15:1093–1100.

Soman, J., T. Tao, and G. N. Phillips. 1999. Conformational variation of calcium-bound troponin C. *Proteins.* 37:510–511.

Spudich, J. A., and S. Watt. 1971. The regulation of rabbit skeletal muscle contraction. Biochemical studies of the interaction of the tropomyosin-troponin complex with actin and the proteolytic fragments of myosin. *J. Biol. Chem.* 246:4866–4871.

Stefancsik, R., P. K. Jha, and S. Sarkar. 1998. Identification and mutagenesis of a highly conserved domain in troponin T responsible for troponin I binding: potential role for coiled coil interaction. *Proc. Natl. Acad. Sci. U.S.A.* 95:957–962.

Stone, D. B., P. A. Timmins, D. K. Schneider, I. Krylova, C. H. I. Ramos, F. C. Reinach, and R. A. Mendelson. 1998. The effect of regulatory Ca^{2+} on the in situ structures of troponin C and troponin I: a neutron scattering study. *J. Mol. Biol.* 281:689–704.

Stryer, L. 1978. Fluorescence energy transfer as a spectroscopic ruler. *Annu. Rev. Biochem.* 47:819–846.

Strynadka, N. C. J., M. Cherney, A. R. Sielecki, M. X. Li, L. B. Smillie, and M. N. G. James. 1997. Structural details of a calcium-induced molecular switch: x-ray crystallographic analysis of the calcium-saturated N-terminal domain of troponin C at 1.75 Å resolution. *J. Mol. Biol.* 273:238–255.

Sundaralingam, M., R. Bergstrom, G. Strasburg, S. T. Rao, M. Greaser, and B. C. Wang. 1985. Molecular structure of troponin C from chicken skeletal muscle at 3 Å resolution. *Science.* 227:945–948.

Syska, H., J. M. Wilkinson, R. J. A. Grand, and S. V. Perry. 1976. The relationship between biological activity and primary structure of troponin I from white skeletal muscle of the rabbit. *Biochem. J.* 153:375–387.

Talbot, J. A., and R. S. Hodges. 1981. Synthetic studies of the inhibitory region of rabbit skeletal troponin I. *J. Biol. Chem.* 256:2798–2802.

Tao, T. 1978. Nanosecond fluorescence depolarization studies on actin labeled with 1,5-IAEDANS and dansyl chloride. *FEBS Lett.* 93: 146–150.

Tao, T., and J. Cho. 1979. Fluorescence lifetime quenching studies on the accessibilities of actin sulfhydryl sites. *Biochemistry.* 18:2759–2765.

Tao, T., B. J. Gong, Z. Grabarek, and J. Gergely. 1999. Conformational changes induced in troponin I by interaction with troponin T and actin/tropomyosin. *Biochim. Biophys. Acta.* 1450:423–433.

Tao, T., B.-J. Gong, and P. C. Leavis. 1990. Calcium-induced movement of troponin-I relative to actin in skeletal muscle thin filaments. *Science.* 247:1265–1372.

Tao, T., E. Gowell, G. M. Strasburg, J. Gergely, and P. C. Leavis. 1989. Ca^{2+} dependence of the distance between Cys-98 of troponin C and Cys-133 of troponin I in the ternary troponin complex: resonance energy transfer measurements. *Biochemistry.* 28:5902–5908.

Tao, T., M. L. Lamkin, and S. S. Lehrer. 1983. Excitation energy transfer studies of the proximity between tropomyosin and actin in reconstituted skeletal muscle thin filaments. *Biochemistry.* 22:3059–3066.

Tao, T., M. Lamkin, and C. J. Scheiner. 1985. The conformation of the C-terminal region of actin: a site-specific photo-cross-linking study using benzophenone-4-maleimide. *Arch. Biochem. Biophys.* 240: 627–634.

Tobacman, L. S. 1996. Thin filament-mediated regulation of cardiac contraction. *Annu. Rev. Physiol.* 58:447–481.

Tripet, B., J. E. Van Eyk, and R. S. Hodges. 1997. Mapping of a second actin-tropomyosin and a second troponin C binding site within the C terminus of troponin I, and their importance in the Ca^{2+}-dependent regulation of muscle contraction. *J. Mol. Biol.* 271:728–750.

Van Eyk, J. E., L. T. Thomas, B. Tripet, R. J. Wiesner, J. R. Pearlstone, C. S. Farah, F. C. Reinach, and R. S. Hodges. 1997. Distinct regions of troponin I regulate Ca^{2+}-dependent activation and Ca^{2+} sensitivity of the acto-S1-Tm ATPase activity of the thin filament. *J. Biol. Chem.* 272:10529–10537.

Vassylyev, D. G., S. Takeda, S. Wakatsuki, K. Maeda, and Y. Maeda. 1998. Crystal structure of troponin C in complex with troponin I fragment at 2.3 Å resolution. *Proc. Natl. Acad. Sci. U.S.A.* 95:4847–4852.

Wang, Z., J. Gergely, and T. Tao. 1992. Characterization of the Ca^{2+}-triggered conformational transition in troponin C. *Proc. Natl. Acad. Sci. U.S.A.* 89:11814–11817.

Wang, Z., S. Sarkar, J. Gergely, and T. Tao. 1990. Ca^{2+}-dependent interactions between the C-Helix of troponin-C and troponin-I. Photo-cross-linking and fluorescence studies using a recombinant troponin-C. *J. Biol. Chem.* 265:4953–4957.